INTECH
open science | open minds

OPEN ACCESS
ARTICLE

International Journal of Advanced Robotic Systems

Research on the Cross-Coupling of a Two Axes Gimbal System with Dynamic Unbalance

Regular Paper

Maher Abdo[1,*], Ahmad Reza Vali[1], Alireza Toloei[2] and Mohammad Reza Arvan[1]

1 Control Department, Electrical Engineering Faculty, MUT, Tehran, Iran
2 Aerospace Department, Shaid Beheshti University, Tehran, Iran
* Corresponding author E-mail: maherabdo74@yahoo.com

Received 09 Dec 2012; Accepted 09 Jul 2013

DOI: 10.5772/56963

Abstract The aim of the gimballed stabilization system is to stabilize the sensor's line of sight towards a target by isolating the sensor from the disturbance induced by the operating environment, such as various disturbance torques and body motions. This paper presents a two axes gimbal assembly. The torque relationships are derived considering the angular motion of the base body and the dynamic unbalance. The stabilization loops for the two axes gimbal system are constructed and related to each other with a cross-coupling unit. Next, the overall model is simulated using two approaches and the obtained results are compared to show the correction of the model proposed. Finally, numerous tests are applied to evaluate the model's performance and investigate the effects of torque disturbance considered in this research.

Keywords Gimbal System, Line of Sight, Rate Gyro, Inertia Stabilization System, Stabilization Loop

1. Introduction

Optical equipment (such as IR, radar, laser, and television) has seen wide use in many important applications, such as image processing, guided missiles, tracking systems and navigation systems. In such systems, the optical sensor axis must be accurately pointed from a movable base to a fixed or moving target. Therefore, the sensor's line of sight (LOS) must be strictly controlled. In such an environment, where the equipment is typically mounted on a movable platform, maintaining sensor orientation towards a target is a serious challenge. An inertial stabilization platform (ISP) is an appropriate way of solving this challenge [1]. Usually, a two axes gimbal system is used to provide stabilization to the sensor while different disturbances affect it. The most important disturbance sources are the base's angular motion, the dynamics of the gimballed system and the gimbal mass unbalance. It is therefore necessary to capture all the dynamics of the plant and express it in analytical form before the design of the gimbal assembly is taken up [2]. The performance of a system depends heavily on the accuracy of plant modelling. A typical plant for such problems consists of an electro-mechanical gimbal assembly with angular freedom in one, two or three axes and one or more EO sensors [3]. The two axes gimbal model has been discussed in many studies using

different assumptions and methods. In [4], the kinematics and geometrical coupling relationships for the two degrees of freedom gimbal assembly have been obtained for a simplified case when each gimbal is balanced and the gimballed elements bodies are suspended about their principal axes. Equations of motion for the two axes gimbal configuration have been discussed on the assumption that the gimbals are rigid bodies and have no mass unbalance [5]. Extrand has shown that inertia disturbances can be eliminated by certain inertia symmetry conditions, and that certain choices of inertia parameters can eliminate the inertia cross-couplings between the channels of the gimbal system [5]. Neither of the studies [4, 5] mentioned above have been simulated. A single degree of freedom (SDOF) gimbal operating in a complex vibration environment has been presented by Daniel in [6]. It has been illustrated how the vibrations excite both static and dynamic unbalance disturbance torques, which can be eliminated by statically and dynamically balancing the gimbal, though it is regarded costly and time consuming [6]. A novel method to measure unbalanced moments in a two axes gimballed seeker has been presented by Yu and Zhao in [7], but this method was inadequate for the better performance of a seeker owing to the limited sensor's own accuracy. In [8], a proxy-based sliding mode was applied on a two axes gimbal system, where its motion equations were derived on the assumptions that gimbals have no dynamic mass imbalance and that the mass distribution of the gimbals is symmetrical with respect to the frame axes under consideration. In addition, the effects of the base angular velocities were not highlighted. In [9], a two axes gimbal mechanism was introduced with just the modelling of the azimuth axis focused upon - the elevation angle was kept fixed and the cross moments of inertia were taken to be zero. In both [5] and [10], the dynamical model of the elevation and azimuth gimbals was derived on the assumption that the gimbals' mass distribution was symmetrical with respect to their frame axes. Therefore, the products of inertia were neglected and the model was simplified. It is clear that two axes gimbal systems have been studied in many papers and that the gimbal system model has been obtained utilizing different approaches. However, most of these studies have considered that the elevation and azimuth channels are identical such that one axis was simulated and tested. Thus, the cross-coupling - which is caused by the base angular motion and the properties of gimbal system dynamics – has been ignored. Moreover, it has been supposed that the gimbals' mass distribution is symmetrical such that the gimbals have no dynamic mass unbalance. Therefore, this article is devoted to the presentation of a model of a two axes gimbal system in order to simplify the picture of the gimbal systems and further investigate the properties of this configuration by taking into account the most important disturbance sources, such as the base rotations, the gimbal system imperfections and the gimbal system properties. In another words, the motivation and importance of this research results from deriving the torque relationships by considering the angular motion of the base body and the dynamic mass unbalance, and then introducing the overall control system with cross-coupling. This is what can provide more understanding of the activity of such systems wherever they are designed considering the most important work conditions. The remainder of this paper is organized as follows. The equations of the gimbals motion are derived using Newton's second law, considering the angular motion of the base body, the cross-coupling between gimbals, and the unsymmetrical gimbals mass' distribution. Afterwards, the stabilization loop is investigated and constructed. The system is modelled using MATLAB/Simulink and MATLAB/SimMechanics, and their results are compared to verify the present model. The obtained model is tested for many different scenarios to demonstrate the effects of disturbance torques caused by the base angular motion and the dynamic mass unbalance. Finally, the results are discussed, concluding remarks are made, and some future works are suggested so as to develop this research.

2. Problem formulation

The stabilization is usually provided to the sensor by suspending it on the inner gimbal of a two axes gimbal system, as is shown in figure 1.

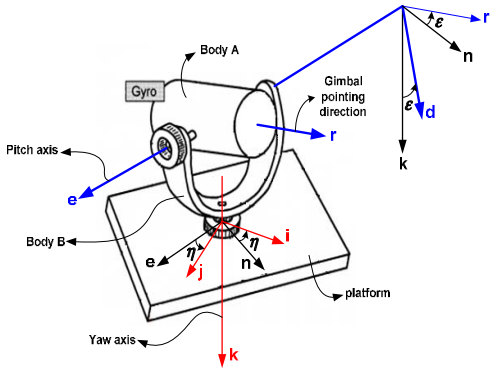

Figure 1. The two axes gimbal system.

Furthermore, a rate gyro located on the inner gimbal is utilized to measure the angular rates in the two planes of interest. The gyro outputs are used as feedback to torque motors related to the gimbals. The overall control system is constructed utilizing two identical stabilization loops (figure 2) for the inner (elevation) and outer (azimuth) gimbals. This system aims to isolate the stabilized object (sensor) from the base rotation. Therefore, the elevation gimbal's angular velocities, which are the outputs of the control system, must be made zero. In other words, the sensor optical axis must be maintained as non-rotating in an inertial space despite torque disturbances.

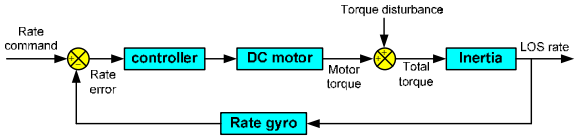

Figure 2. The one axis gimbal stabilization loop.

The two control loops in the elevation and azimuth channels are related to each other by the cross-coupling unit, which is built based on the relationships of the torques affected on the two gimbals. The cross-coupling expresses the properties of the gimbal system dynamics. It reflects the fact that the azimuth gimbal can affect the elevation gimbal even when the base body is non-rotating. In addition, there is similar impact on the part of the elevation gimbal on the azimuth gimbal. As a result, the cross-coupling may be defined as the effect on one axis by the rotation of another [6]. It is worth mentioning that this paper is based on the following assumptions:

1. The gimbals are rigid bodies. Moreover, the gimbal rotation centre and the frame origin are identical.
2. The gimbal mass centre is supposed to be in the common centre of rotation, which means that the gimbals have no static mass unbalance.
3. The gimbal mass distribution is not symmetrical with respect to the gimbal frame axes, which means that the gimbals have dynamic mass unbalance

3. Dynamic mass unbalance and kinematic coupling

The dynamic mass unbalance is the result of a non-symmetrical mass distribution called the 'product of inertia' (POI) [6]. The dynamic unbalance concept can be indicated by the inertia matrix. Therefore, if the considered gimbal has a symmetrical mass distribution with respect to its frame axes, then the gimbal has no dynamic unbalance and its inertia matrix is diagonal. In addition, and on the one hand, if the gimbal has a non-symmetrical mass distribution with respect to its frame axes, then the gimbal has dynamic unbalance and its inertia matrix is not diagonal. On the other hand, the gimbal assembly provides the connection between the system base and the line of sight (LOS). Therefore, to practically estimate the system performance, the mechanisms that couple the base motion and the LOS angular motion must be completely evaluated. Next, it will be shown that the angular rate coupling is caused by the kinematic relationships between the gimbal assembly parameters and the base motions.

4. Reference frames and notations

In this paper, a two axes gimbal system depicted in figure 1 is considered. Three reference frames are identified as follows. Frame P fixed to the fuselage body with axes (i,j,k), frame B fixed to the azimuth (outer) gimbal with axes (n,e,k), and frame A fixed to the elevation (inner) gimbal with axes (r,e,d). The r-axis coincides with the sensor optical axis. The k axis points "downwards". The centre of rotation is at the frame origin, which is assumed to be the same point for the three frames. The transformation matrices are based on the angles of rotation ε and η:

$$ {}^{B}_{P}C = \begin{bmatrix} \cos\eta & \sin\eta & 0 \\ -\sin\eta & \cos\eta & 0 \\ 0 & 0 & 1 \end{bmatrix} \tag{1} $$

$$ {}^{A}_{B}C = \begin{bmatrix} \cos\varepsilon & 0 & -\sin\varepsilon \\ 0 & 1 & 0 \\ \sin\varepsilon & 0 & \cos\varepsilon \end{bmatrix} \tag{2} $$

${}^{B}_{P}C$ is the transformation from frame P to frame B. Similarly, ${}^{A}_{B}C$ is the transformation from frame B to frame A. The inertial angular velocity vectors of frames P, B and A, respectively, are:

$$ {}^{P}\bar{\omega}_{P/I} = \begin{bmatrix} \omega_{pi} \\ \omega_{pj} \\ \omega_{pk} \end{bmatrix}, {}^{B}\bar{\omega}_{B/I} = \begin{bmatrix} \omega_{Bn} \\ \omega_{Be} \\ \omega_{BK} \end{bmatrix}, {}^{A}\bar{\omega}_{A/I} = \begin{bmatrix} \omega_{Ar} \\ \omega_{Ae} \\ \omega_{Ad} \end{bmatrix} \tag{3} $$

where $\omega_{p_i}, \omega_{p_j}, \omega_{p_k}$ are the body angular velocities of frame P in relation to the inertial space about the i, j and k axes respectively, $\omega_{B_n}, \omega_{B_e}, \omega_{B_k}$ are the azimuth gimbal's angular velocities in relation to the inertial space about the n, e and k axes respectively, and $\omega_{A_r}, \omega_{A_e}, \omega_{A_d}$ are the elevation gimbal's angular velocities in relation to the inertial space about the r, e and d axes respectively. The inertia matrices of the elevation and azimuth gimbals are:

$$ {}^{A}J_{inner} = \begin{bmatrix} A_r & A_{re} & A_{rd} \\ A_{re} & A_e & A_{de} \\ A_{rd} & A_{de} & A_d \end{bmatrix} \tag{4} $$

$$ {}^{B}J_{outer} = \begin{bmatrix} B_n & B_{ne} & B_{nk} \\ B_{ne} & B_e & B_{ke} \\ B_{nk} & B_{ke} & B_k \end{bmatrix} \tag{5} $$

Where A_r, A_e, A_d are the elevation gimbal moments of inertia about the r, e and d axes, A_{re}, A_{rd}, A_{de} are the elevation gimbal moments products of inertia, B_n, B_e, B_k are the azimuth gimbal moments of inertia about the n, e and k axes, and B_{ne}, B_{nk}, B_{ke} are the azimuth gimbal moments' products of inertia. Additionally, T_{EL} is introduced as the total external torque about the elevation gimbal e-axis, and T_{AZ} as the total external torque about the azimuth gimbal k-axis. As mentioned above, the aim is to stabilize the gimbal system LOS (r-axis), which means that the angular velocities ω_{Ae} and ω_{Ad} must be equal to

zero. ω_{Ae} and ω_{Ad} can be measured by a rate gyro placed on the elevation gimbal. In general, Euler angles define the position between two related reference frames [7]. For the body's fixed frame P and the azimuth gimbal frame B with one angle, η, utilizing this principle, the following relation can be obtained:

$$\begin{aligned} \omega_{Bn} &= \omega_{Pi}\cos\eta + \omega_{Pj}\sin\eta \quad (a)\\ \omega_{Be} &= -\omega_{Pi}\sin\eta + \omega_{Pj}\cos\eta \quad (b)\\ \omega_{BK} &= \omega_{Pk} + \dot{\eta} \quad (c) \end{aligned} \tag{6}$$

Similarly, between the azimuth gimbal frame B and the elevation gimbal frame A, we have:

$$\begin{aligned} \omega_{Ar} &= \omega_{Bn}\cos\varepsilon - \omega_{BK}\sin\varepsilon \quad (a)\\ \omega_{Ae} &= \omega_{Be} + \dot{\varepsilon} \quad (b)\\ \omega_{Ad} &= \omega_{Bn}\sin\varepsilon + \omega_{Bk}\cos\varepsilon \quad (c) \end{aligned} \tag{7}$$

5. Equations for the gimbals' motion using Newton's second law (without dynamic unbalance)

Newton's first law applied to rotational motion asserts that a body does not accelerate with respect to an inertial frame unless a torque is applied. Furthermore, Newton's second law establishes that if a net torque T is applied to a homogenous rigid mass with a moment of inertia J, then the body develops an angular acceleration α [11] according to:

$$T = J.\alpha \tag{8}$$

Therefore, in principle, all that is required to prevent an object from rotating with respect to an inertial space is to ensure that the applied torque is zero [11]. However, despite careful electromechanical design, numerous sources of torque disturbances can act on a real mechanism causing the excessive motion or jitter of the LOS [11]. The basic equations of motion for the azimuth and elevation gimbals are directly obtained if the gimbals are considered as rigid bodies. Therefore, the external torques applied to the gimbal are:

$$\bar{T} = \frac{d}{dt}\bar{H} + \bar{\omega}\times\bar{H} \;\; ; \;\; \bar{H} = J.\bar{\omega} \tag{9}$$

where J is the inertia matrix, $\bar{\omega}$ is the angular velocity of the gimbal, and $\bar{H}$ is the angular momentum [5]. From these relationships, the y and z components of the gimbal's motion are obtained.

5.1 Elevation channel relationships

The angular momentum for the elevation gimbal, which is considered as a rigid body, is:

$${}^{A}\bar{H}_{inner} = {}^{A}J_{inner}\bar{\omega}_{A/I} = \begin{bmatrix} A_r\omega_{Ar} + A_{re}\omega_{Ae} + A_{rd}\omega_{Ad} \\ A_{re}\omega_{Ar} + A_e\omega_{Ae} + A_{de}\omega_{Ad} \\ A_{rd}\omega_{Ar} + A_{de}\omega_{Ae} + A_d\omega_{Ad} \end{bmatrix} = \begin{bmatrix} H_r \\ H_e \\ H_d \end{bmatrix} \tag{10}$$

The moment equation for a rotating frame is:

$$\bar{T} = \left.\frac{d\bar{H}_{inner}}{dt}\right|_A + \bar{\omega}_A \times \bar{H}_{inner} \tag{11}$$

$$\bar{T} = \begin{bmatrix} \dot{H}_r + \omega_{Ae}H_d - \omega_{Ad}H_e \\ \dot{H}_e + \omega_{Ad}H_r - \omega_{Ar}H_d \\ \dot{H}_d + \omega_{Ar}H_e - \omega_{Ae}H_r \end{bmatrix} \tag{12}$$

The total external torque about the elevation gimbal e-axis is:

$$T_{EL} = \dot{H}_e + \omega_{Ad}H_r - \omega_{Ar}H_d \tag{13}$$

This equation can be obtained as a differential equation for the elevation angular velocity:

$$\begin{aligned} A_e\dot{\omega}_{Ae} &= T_{EL} + T_{D-EL} \\ T_{D-EL} &= (A_d - A_r)\omega_{Ar}\omega_{Ad} - A_{re}(\dot{\omega}_{Ar} + \omega_{Ae}\omega_{Ad}) \\ &\quad + A_{rd}(\omega_{Ar}^2 - \omega_{Ad}^2) - A_{de}(\dot{\omega}_{Ad} - \omega_{Ae}\omega_{Ar}) \end{aligned} \tag{14}$$

All the inertia terms on the right-hand side of (14), which are denoted by T_{D-EL}, constitute unwanted disturbances that enter the control system as external torque disturbances. Using (7), this disturbance term T_{D-EL} can be written as $T_{D-EL} = T_{B-EL} + T_{C-EL}$, whereas:

$$\begin{aligned} T_{B-EL} &= -(A_{de}\sin\varepsilon + A_{re}\cos\varepsilon)(\dot{\omega}_{Bn} + \omega_{Be}\omega_{Bk}) \\ &\quad + (A_{de}\cos\varepsilon - A_{re}\sin\varepsilon)\omega_{Bn}\omega_{Be} \\ &\quad + [(A_d - A_r)\cos(2\varepsilon) - 2A_{rd}\sin(2\varepsilon)]\omega_{Bn}\omega_{Bk} \\ &\quad + \frac{1}{2}[(A_d - A_r)\sin(2\varepsilon) + 2A_{rd}\cos(2\varepsilon)]\omega_{Bn}^2 \end{aligned} \tag{15}$$

$$\begin{aligned} T_{C-EL} &= (A_{re}\sin\varepsilon - A_{de}\cos\varepsilon)\dot{\omega}_{Bk} \\ &\quad - \frac{1}{2}[(A_d - A_r)\sin(2\varepsilon) + 2A_{rd}\cos(2\varepsilon)]\omega_{Bk}^2 \end{aligned} \tag{16}$$

To highlight the concept of cross-coupling, it is assumed that the base is non-rotating, $\omega_{pi} = \omega_{pj} = \omega_{pk} = 0$. Thus, from (6) we obtain $\omega_{Bn} = \omega_{Be} = 0$ and, by that, $T_B = 0$. However, ω_{Bk} and, consequently, T_{C-EL}, are not necessarily zero for this case; the azimuth gimbal's motion may influence the elevation gimbal via T_{C-EL} even for a non-rotating body. Therefore, T_{C-EL} is labelled as the cross-coupling term. When it is supposed that the elevation gimbal has no dynamic unbalance (i.e., $A_{re} = A_{rd} = A_{de} = 0$) equation (14) becomes:

$$A_e\dot{\omega}_{Ae} = T_{EL} + (A_d - A_r)\omega_{Ar}\omega_{Ad} = T_{EL} + T_{D-EL} \tag{17}$$

Inserting equations (7-a) and (7-c) in (17) gives:

$$\begin{aligned} A_e\dot{\omega}_{Ae} &= T_{EL} + T_{D-EL1} + T_{D-EL2} \; ; \\ T_{D-EL1} &= -(A_d - A_r)\omega_{Ad}^2\tan(\varepsilon) \\ T_{D-EL2} &= \omega_{Bn}\omega_{Ad}(A_d - A_r)\left[\frac{1}{\cos\varepsilon}\right] \end{aligned} \tag{18}$$

The equation for the elevation gimbal's motion (18) can be expressed in block diagram form, as shown in figure 3.

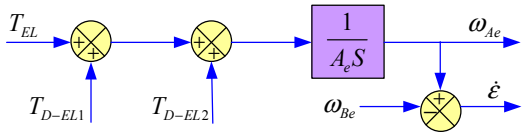

Figure 3. Equation for the elevation gimbal's motion without dynamic unbalance.

5.2 Azimuth channel relationships

The angular momentum of the total gimbal system (expressed in frame B) is the sum of the angular momentum of the elevation and azimuth gimbals:

$$\bar{H} = \begin{bmatrix} H_i \\ H_j \\ H_k \end{bmatrix} = {}^{B}J_{outer}\bar{\omega}_{B/I} + {}^{A}_{B}C^{T}\,{}^{A}J_{inner}\bar{\omega}_{A/I} \tag{19}$$

The moment equation applied to frame B is:

$$\bar{T} = \frac{d}{dt}\bar{H}\Big|_{B} + \bar{\omega}_{B/I} \times \bar{H} \tag{20}$$

The rotation of the outer (azimuth) gimbal occurs around the k axis. Therefore, the motion equation for the azimuth gimbal is the k-component of the moment equation (20). Thus, the k-component for the two terms in equation (20)'s right-hand side must be computed as follows:

$$\begin{aligned} H_k = {} & B_{nk}\omega_{Bn} + B_{ke}\omega_{Be} + B_k\omega_{Bk} \\ & -(A_r\omega_{Ar} + A_{re}\omega_{Ae} + A_{rd}\omega_{Ad})\sin\varepsilon \\ & +(A_{rd}\omega_{Ar} + A_{de}\omega_{Ae} + A_d\omega_{Ad})\cos\varepsilon \end{aligned} \tag{21}$$

$$\begin{aligned} \left(\bar{\omega}_{B/I} \times \bar{H}\right)_k = {} & \omega_{Bn}(B_{ne}\omega_{Bn} + B_e\omega_{Be} \\ & + B_{ke}\omega_{Bk} + A_{re}\omega_{Ar} + A_e\omega_{Ae} + A_{de}\omega_{Ad}) \\ & - \omega_{Be}(B_n\omega_{Bn} + B_{ne}\omega_{Be} + B_{nk}\omega_{Bk}) \\ & - \omega_{Be}(A_r\omega_{Ar} + A_{re}\omega_{Ae} + A_{rd}\omega_{Ad})\cos\varepsilon \\ & - \omega_{Be}(A_d\omega_{Ar} + A_{de}\omega_{Ae} + A_d\omega_{Ad})\sin\varepsilon \end{aligned} \tag{22}$$

Based on equations (21), (22) and (7) the equation for the azimuth gimbal's motion is:

$$J_{eq}\dot{\omega}_{Bk} = T_{Az} + T_{d1} + T_{d2} + T_{d3} \tag{23}$$

The resulting equation is a differential equation for the azimuth gimbal's angular velocity. Where $T_d = T_{d1} + T_{d2} + T_{d3}$ are a different gimbal inertia disturbances, J_{eq} is the instantaneous moment of inertia about the k-axis. These terms are expressed as follows:

$$\begin{aligned} J_{eq} = {} & B_k + A_r\sin^2\varepsilon + A_d\cos^2\varepsilon \\ & - A_{rd}\sin(2\varepsilon) \end{aligned} \tag{24}$$

$$T_{d1} = \begin{bmatrix} B_n + A_r\cos^2\varepsilon + A_d\sin^2\varepsilon \\ +A_{rd}\sin(2\varepsilon) - (B_e + A_e) \end{bmatrix}\omega_{Bn}\omega_{Be} \tag{25}$$

$$\begin{aligned} T_{d2} = {} & -\begin{bmatrix} B_{nk} + (A_d - A_r)\sin\varepsilon\cos\varepsilon \\ +A_{rd}\cos(2\varepsilon) \end{bmatrix} \\ & \times(\dot{\omega}_{Bn} - \omega_{Be}\omega_{Bk}) \\ & -(B_{ke} + A_{de}\cos\varepsilon - A_{re}\sin\varepsilon) \\ & \times(\dot{\omega}_{Be} + \omega_{Bn}\omega_{Bk}) \\ & -(B_{ne} + A_{re}\cos\varepsilon + A_{de}\sin\varepsilon) \\ & \times(\omega_{Bn}^2 - \omega_{Be}^2) \end{aligned} \tag{26}$$

$$\begin{aligned} T_{d3} = {} & \ddot{\varepsilon}(A_{re}\sin\varepsilon - A_{de}\cos\varepsilon) \\ & +\dot{\varepsilon}[(A_r - A_d)(\omega_{Bn}\cos(2\varepsilon) - \omega_{Bk}\sin(2\varepsilon))] \\ & +\dot{\varepsilon}[2A_{re}(\omega_{Bn}\sin(2\varepsilon) + \omega_{Bk}\cos(2\varepsilon))] \\ & +\dot{\varepsilon}[(A_{de}\sin\varepsilon + A_{re}\cos\varepsilon)(\omega_{Ae} + \omega_{Be}) - A_e\omega_{Bn}] \end{aligned} \tag{27}$$

Using $\dot{\varepsilon} = \omega_{Ae} - \omega_{Be}$, the disturbance T_d can be written as $T_d = T_{b-AZ} + T_{c-AZ}$ whereas

$$\begin{aligned} T_{b-AZ} = {} & T_{d1} + T_{d2} + (A_{de}\cos\varepsilon - A_{re}\sin\varepsilon)\dot{\omega}_{Be} \\ & -(A_{de}\sin\varepsilon + A_{re}\cos\varepsilon)\omega_{Be}^2 \\ & +[(A_r - A_d)\cos(2\varepsilon) + 2A_{rd}\sin(2\varepsilon) - A_e]\dot{\varepsilon}\omega_{Bn} \\ & +[(A_r - A_d)\sin(2\varepsilon) - 2A_{rd}\cos(2\varepsilon)]\omega_{Be}\omega_{Bk} \end{aligned} \tag{28}$$

$$\begin{aligned} T_{c-AZ} = {} & (A_{re}\sin\varepsilon - A_{de}\cos\varepsilon)\dot{\omega}_{Ae} \\ & +(A_{re}\cos\varepsilon + A_{de}\sin\varepsilon)\omega_{Ae}^2 \\ & +[(A_d - A_r)\sin(2\varepsilon) + 2A_{rd}\cos(2\varepsilon)]\omega_{Ae}\omega_{Bk} \end{aligned} \tag{29}$$

Similarly to the elevation gimbal, for a non-rotating body, we have $\omega_{Bn} = \omega_{Be} = 0$ and by that $T_{b-AZ} = 0$. However, irrespective of the base motion, we also have a cross-coupling term T_{c-AZ} influencing the azimuth gimbal from elevation gimbal's motions. In order to convert equation (23) into a differential equation for the elevation angular velocity ω_{Ad} we use equations (7) to obtain ω_{Bk} and its derivative $\dot{\omega}_{Bk}$ as follows:

$$\dot{\omega}_{Bk} = \frac{\dot{\omega}_{Ad} - \dot{\omega}_{Bn}\sin\varepsilon - \omega_{Ar}(\omega_{Ae} - \omega_{Be})}{\cos\varepsilon} \tag{30}$$

Equation (21) becomes:

$$J_{eq}\dot{\omega}_{Ad} = T_{Az}\cos\varepsilon + T_d\cos\varepsilon + T_d' \tag{31}$$

$$T_d' = J_{eq}\left[\dot{\omega}_{Bn}\sin\varepsilon + \omega_{Ar}(\omega_{Ae} - \omega_{Be})\right] \tag{32}$$

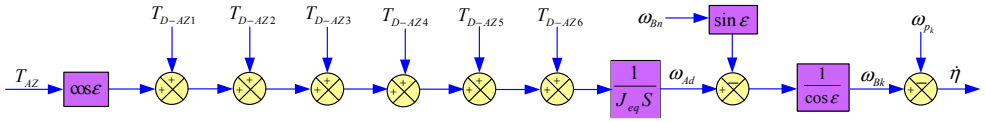

Figure 4. Equation for the azimuth gimbal's motion without dynamic unbalance.

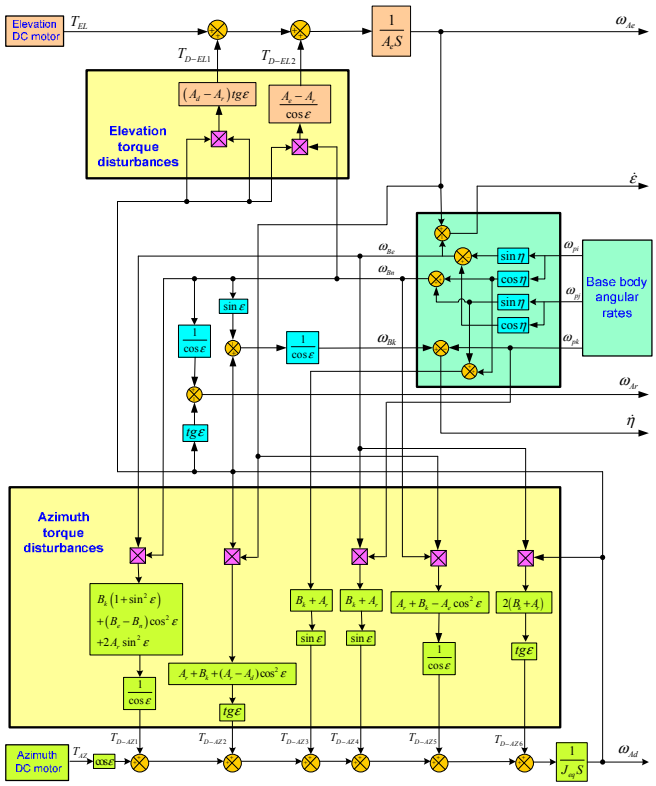

Figure 5. The two axes gimbal torque relationships when the elevation and azimuth gimbals have no dynamic unbalance.

We denote:

$$T_{D-AZ} = T_d \cos\varepsilon + T'_d \tag{33}$$

From equation (6-a), we have:

$$\dot{\omega}_{Bn} = \left(\dot{\omega}_{Pi}\cos\eta + \dot{\omega}_{Pj}\sin\eta\right) + \omega_{Be}\left(\omega_{Bk} - \omega_{Pk}\right) \tag{34}$$

Inserting equations (34) and (7-c) in (31), and supposing that gimbals A and B have no dynamic unbalance (i.e., $A_{re} = A_{rd} = A_{de} = 0$ & $B_{ne} = B_{nk} = B_{ke}$) we get:

$$J_{eq}\dot{\omega}_{Ad} = T_{Az}\cos\varepsilon + T_{D-AZ} \tag{35}$$

where T_{D-AZ} is the sum of the next torques:

$$T_{D-Az1} = \frac{-\omega_{Bn}\omega_{Be}\begin{bmatrix} B_k\left(1+\sin^2\varepsilon\right) + 2A_r\sin^2\varepsilon \\ +\left(B_e - B_n\right)\cos^2\varepsilon \end{bmatrix}}{\cos\varepsilon} \tag{36}$$

$$T_{D-AZ2} = -\omega_{Ad}\omega_{Ae}\left[A_r + B_k + \left(A_r - A_d\right)\cos^2\varepsilon\right]\tan(\varepsilon) \tag{37}$$

$$T_{D-AZ3} = \left(\dot{\omega}_{Pi}\cos\eta + \dot{\omega}_{Pj}\sin\eta\right)\left[B_k + A_r\right]\sin\varepsilon \tag{38}$$

$$T_{D-AZ4} = -\omega_{Be}\omega_{Pk}\left[B_k + A_r\right]\sin\varepsilon \tag{39}$$

$$T_{D-AZ5} = \frac{\omega_{Bn}\omega_{Ae}\left[A_r + B_k - A_e\cos^2\varepsilon\right]}{\cos\varepsilon} \tag{40}$$

$$T_{D-AZ6} = 2\omega_{Ad}\omega_{Be}\left[B_k + A_r\right]\tan(\varepsilon) \tag{41}$$

The equation for the azimuth gimbal's motion (35) can be expressed by a block diagram, as shown in figure 4. Now, utilizing (18) and (35), the global torque relationships of the two axes gimbal system introduced on the assumption that gimbals have no dynamic unbalance can be clarified by a block diagram, as indicated in figure 5.

6. Equations of the gimbals' motion when the gimbals have dynamic unbalance

In this paper, the effects of dynamic unbalance are considered and investigated. Therefore, the equations for the gimbals motion (14, 31) are introduced considering all elements of the elevation and azimuth gimbals' matrices $A_{re} \neq 0, A_{rd} \neq 0, A_{de} \neq 0$ & $B_{ne} \neq 0, B_{nk} \neq 0, B_{ke} \neq 0$. Utilizing the equations of the gimbals inertial rates (6, 7), the terms of the disturbance torque are divided into their separate components.

6.1 Elevation channel relationships

The equation for the motion of the elevation gimbal was obtained above in (14). It can be seen that the elements of the inertia matrix form the disturbance term T_{D-EL}. Using (7), the disturbance term T_{D-EL} is converted to:

$$\begin{aligned}
T_{D-EL} &= -\left(A_{de}\sin\varepsilon + A_{re}\cos\varepsilon\right) \\
&\times\left(\dot{\omega}_{Bn} + \omega_{Be}\frac{\omega_{Ad} - \omega_{Bn}\sin\varepsilon}{\cos\varepsilon}\right) \\
&+\left(A_{de}\cos\varepsilon - A_{re}\sin\varepsilon\right)\left(\omega_{Bn}\omega_{Be} - \dot{\omega}_{Bk}\right) \\
&+\frac{\omega_{Bn}\left[\left(A_d - A_r\right)\cos(2\varepsilon)\right]\left(\omega_{Ad} - \omega_{Bn}\sin\varepsilon\right)}{\cos\varepsilon} \\
&+\frac{\omega_{Bn}\left[-2A_{rd}\sin(2\varepsilon)\right]\left(\omega_{Ad} - \omega_{Bn}\sin\varepsilon\right)}{\cos\varepsilon} \\
&+\frac{1}{2}\left[\left(A_d - A_r\right)\sin(2\varepsilon) + 2A_{rd}\cos(2\varepsilon)\right]\omega^2{}_{Bn} \\
&-\frac{1}{2}\left[\left(A_d - A_r\right)\sin(2\varepsilon) + 2A_{rd}\cos(2\varepsilon)\right] \\
&\times\left[\frac{\omega^2{}_{Ad} - 2\omega_{Ad}\omega_{Bn}\sin\varepsilon + \omega^2{}_{Bn}\sin^2\varepsilon}{\cos^2\varepsilon}\right]
\end{aligned} \tag{42}$$

From equation (6), we have:

$$\begin{aligned}
\dot{\omega}_{Bn} &= \left(\dot{\omega}_{Pi}\cos\eta + \dot{\omega}_{Pj}\sin\eta\right) \\
&+\frac{\omega_{Be}\left[\omega_{Ad} - \omega_{Bn}\sin\varepsilon\right]}{\cos\varepsilon} - \omega_{Be}\omega_{Pk}
\end{aligned} \tag{43}$$

$$\dot{\omega}_{Bk} = \dot{\omega}_{Pk} + \ddot{\eta} \tag{44}$$

Inserting equations (43) and (44) in (42), the disturbance term can be formulated as follows:

$$\begin{aligned}
T_{D-EL} &= T_{D-EL1} + T_{D-EL2} + T_{D-EL3} \\
&+ T_{D-EL4} + T_{D-EL5} + T_{D-EL6} + T_{D-EL7} \\
&+ T_{D-EL8} + T_{D-EL9} + T_{D-EL10}
\end{aligned} \tag{45}$$

$$\begin{aligned}
T_{D-EL1} &= \left(A_{de}\sin\varepsilon + A_{re}\cos\varepsilon\right) \\
&\times\begin{bmatrix}\dfrac{-2\omega_{Be}\omega_{Ad} - 2\omega_{Be}\omega_{Bn}\sin\varepsilon}{\cos\varepsilon} \\ +\omega_{Be}\omega_{p_k} - \dot{\omega}_{p_i}\cos\eta + \dot{\omega}_{p_j}\sin\eta\end{bmatrix}
\end{aligned} \tag{46}$$

$$T_{D-EL2} = \omega_{Be}\omega_{Bn}\left(A_{de}\cos\varepsilon - A_{re}\sin\varepsilon\right) \tag{47}$$

$$\begin{aligned}
T_{D-EL3} &= \left(A_d - A_r\right)\left[2\cos\varepsilon - \frac{1}{\cos\varepsilon}\right] \\
&\times\left[\omega_{Bn}\omega_{Ad} - \omega^2{}_{Bn}\sin\varepsilon\right]
\end{aligned} \tag{48}$$

$$T_{D-EL4} = -4A_{rd}\omega_{Bn}\omega_{Ad}\sin\varepsilon \tag{49}$$

$$T_{D-EL5} = 2A_{rd}\omega_{Bn}\omega_{Ad}\tan^2(\varepsilon) \tag{50}$$

$$T_{D-EL6} = A_{rd}\omega^2{}_{Ad}\left[\frac{1}{\cos^2\varepsilon} - 2\right] \tag{51}$$

$$T_{D-EL7} = \left(\dot{\omega}_{p_k} + \ddot{\eta}\right)\left[A_{re}\sin\varepsilon - A_{de}\cos\varepsilon\right] \tag{52}$$

$$T_{D-EL8} = A_{rd}\omega^2_{Bn}\left[-2\sin^2\varepsilon + \tan^2(\varepsilon)\right] \tag{53}$$

$$T_{D-EL9} = \left(A_d - A_r\right)\sin\varepsilon\cos\varepsilon + 2A_{rd}\omega^2_{Bn} \tag{54}$$

$$T_{D-EL10} = \left(A_d - A_r\right)\begin{bmatrix}2\omega_{Ad}\omega_{Bn}\sin\varepsilon \\ -\omega^2_{Ad} - \omega^2_{Bn}\sin^2\varepsilon\end{bmatrix}\tan(\varepsilon) \tag{55}$$

The equation for the elevation gimbal's motion based on the assumption that it has dynamic unbalance can be expressed in block diagram form, as shown in figure 6.

6.2 Azimuth channel relationships

The total external torque about the azimuth gimbal k-axis was denoted by T_{D-AZ} in equation (33). It consists of four components $\left(T_{d1}, T_{d2}, T_{d3}, T'_d\right)$. The term T_{d1} will be denoted as T_{D-AZ1}. Using ω_{Bk} from (7-c), $\dot{\omega}_{Bn}$ from (43) and $\dot{\omega}_{Be}$ from (6-b), the term T_{d2} becomes:

$$\begin{aligned}
T_{D-AZ2} &= \left[B_{nk} + \left(A_d - A_r\right)\sin\varepsilon\cos\varepsilon + A_{rd}\left(2\cos^2\varepsilon - 1\right)\right] \\
&\times\left(-\dot{\omega}_{p_j}\sin\eta - \dot{\omega}_{p_i}\cos\eta + \omega_{Be}\omega_{p_k}\right) \\
&-\left(B_{ke} + A_{de}\cos\varepsilon - A_{re}\sin\varepsilon\right) \\
&\times\left(\dot{\omega}_{p_j}\cos\eta - \dot{\omega}_{p_i}\sin\eta + \omega_{Bn}\omega_{p_k}\right) \\
&-\left(B_{ne} + A_{re}\cos\varepsilon + A_{de}\sin\varepsilon\right)\left(\omega^2_{Bn} - \omega^2_{Be}\right)
\end{aligned} \tag{56}$$

Next, using equations (7-b) and (7-c), the term T_{d3} can be given as follows:

$$\begin{aligned}
T_{D-AZ3} &= \dot{\omega}_{Ae}\left(A_{re}\sin\varepsilon - A_{de}\cos\varepsilon\right) + \left(A_{de}\cos\varepsilon - A_{re}\sin\varepsilon\right) \\
&\times\left(\dot{\omega}_{p_j}\cos\eta - \dot{\omega}_{p_i}\sin\eta\right) + \omega_{Ad}\omega_{Bn}\left(A_{de} - A_{re}\tan(\varepsilon)\right) \\
&+\omega^2_{Bn}\left(A_{re}\tan(\varepsilon) - A_{de}\right)\sin\varepsilon + 2\omega_{Ad}\omega_{Be}\left(A_r - A_d\right)\sin\varepsilon \\
&+\omega_{Ae}\omega_{Bn}\left(A_r - A_d\right) + 2A_{re}\omega_{Ad}\left(\omega_{Ae} - \omega_{Be}\right)\left(2\cos\varepsilon - \frac{1}{\cos\varepsilon}\right) \\
&+\left(\omega_{Ae} - \omega_{Be}\right)\left[\left(A_{de}\sin\varepsilon + A_{re}\cos\varepsilon\right)\left(\omega_{Ae} + \omega_{Be}\right) - A_e\omega_{Bn}\right] \\
&+2A_{re}\left(\omega_{Ae} - \omega_{Be}\right)\omega_{Bn}\tan(\varepsilon)
\end{aligned} \tag{57}$$

From equation (7-a), we have:

$$\omega_{Ar} = -\omega_{Ad}\tan(\varepsilon) + \frac{\omega_{Bn}}{\cos\varepsilon} \tag{58}$$

In addition, using ω_{Bk} from (7-c), $\dot{\omega}_{Bn}$ from (43) and ω_{Ar} from (58), the term T'_d becomes:

$$\begin{aligned}
T_{D-AZ4} &= J_{eq}\left[-\omega_{Be}\omega_{Bn}\left(\frac{1+\sin^2\varepsilon}{\cos\varepsilon}\right) - \omega_{Ad}\omega_{Ae}\tan(\varepsilon)\right. \\
&+\left(\dot{\omega}_{p_i}\cos\eta + \dot{\omega}_{p_j}\sin\eta\right)\sin\varepsilon \\
&\left.-\omega_{Be}\omega_{p_k}\sin\varepsilon + \frac{\omega_{Ae}\omega_{Bn}}{\cos\varepsilon} + 2\omega_{Ad}\omega_{Be}\tan(\varepsilon)\right]
\end{aligned} \tag{59}$$

The equation for the azimuth gimbal's motion based on the assumption that it has dynamic unbalance is shown in figure 7. Utilizing equations (45, 56, 57, 59), the torque relationships of the two axes gimbal system introduced on the assumption that the gimbals have dynamic unbalance can be represented in figure 8.

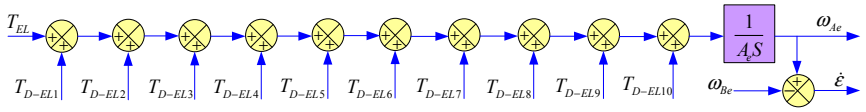

Figure 6. Equation for the elevation gimbal's motion with dynamic unbalance.

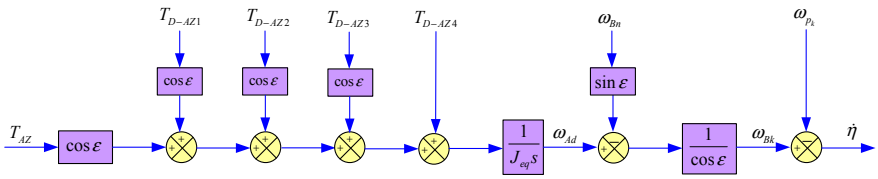

Figure 7. Equation for the azimuth gimbal's motion with dynamic unbalance.

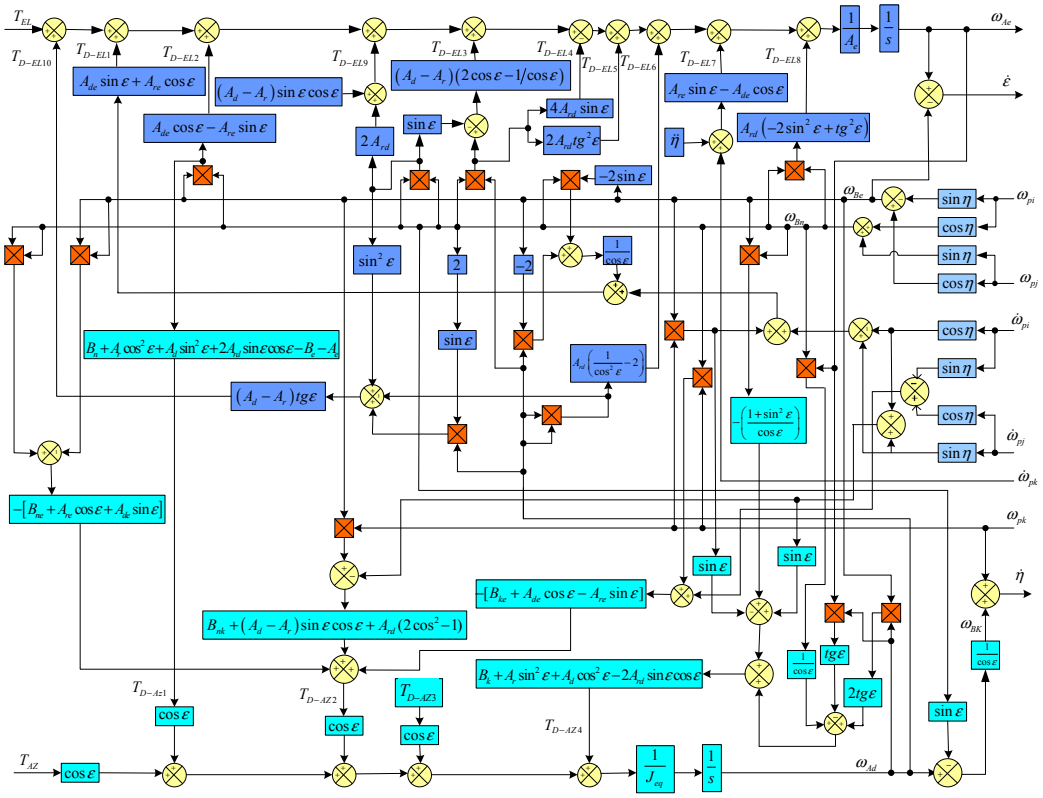

Figure 8. The two axes gimbal torque relationships when the elevation and azimuth gimbals have dynamic unbalance.

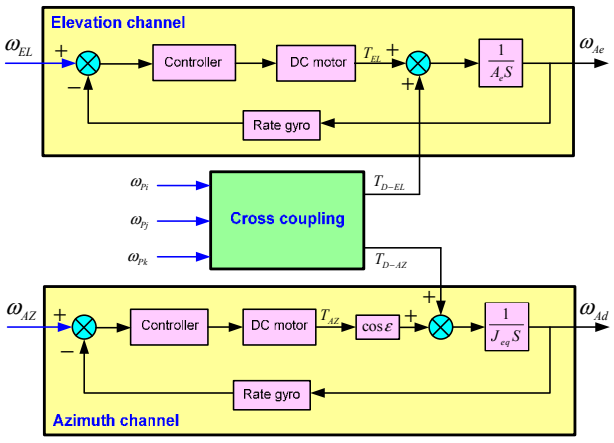

Figure 9. The elevation and azimuth stabilization loops.

7. Simulation and results

The control system of the two axes gimbal assembly consists of two stabilization loops with a cross-coupling unit relating them. Every loop is constructed using a PI controller, a DC motor and a rate gyro in the feedback. The overall simulation model of the gimbal system is prepared in the MATLAB/Simulink environment, as depicted in figure 9.

Although, the researchers tried to utilize and apply many different modern techniques to control the gimbal systems, the conventional PID and its constructors are still the most used approach due to their simple structure, cheap cost, simple design and high performance [12]. Therefore, a PI controller has been utilized in each channel, as follows:

$$K_{EL}(s)=0.09+\frac{12.5}{s}\ ,\ K_{AZ}(s)=0.5+\frac{12.5}{s} \qquad (60)$$

The direct current (DC) motor is one of the simplest motor types. It is widely preferred for high performance systems requiring minimum torque ripple, rapid dynamic torque, speed responses, high efficiency and good inertia [13]. The specifications of the DC motor that was used are displayed in table 1.

Parameter	Value
Nominal voltage u_a	27 V
No load speed ω_{nL}	303 rpm
Terminal resistance R_a	4.5 Ω
Terminal inductance L_a	0.003 H
Torque constant K_{TM}	0.85 Nm/A
Back EMF K_e	0.85 V/rad/sec
Rotor inertia J_m	0.0017 Kgm²
Damping ratio a_m	0

Table 1. The DC motor's specifications.

The transfer function of the DC motor is given by:

$$G_m(s)=\frac{K_{TM}}{(L_a s+R_a)\cdot(J_m^* s+a_m^*)+K_e K_{TM}}=\frac{24637.68}{s^2+1500s+20942} \qquad (61)$$

The angular rates of the inner gimbal are measured by a tow axes rate gyro. Table 2 indicates the utilized gyro specifications. The rate gyro can typically be modelled in the second-order system. It is assumed that the gyro's natural frequency $\omega_n = 50\,Hz$, and that the damping ratio $\zeta = 0.7$.

Input rate	From ± 40 to ±1000 °/sec
Output	AC or DC
Scale factor	Customer specification
Natural frequency	20 to 140 Hz
Damping ratio	0.4 to 1.0

Table 2. The gyroscope's characteristics.

Thus, the transfer function of the gyro is:

$$G_{Gyro}(s)=\frac{\omega_n^2}{(s^2+2\zeta\omega_n s+\omega_n^2)}=\frac{2500}{(s^2+70s+2500)} \qquad (62)$$

The values of the inertia matrices for the elevation and azimuth gimbals are:

$$^{A}J_{inner}=\begin{bmatrix}0.001 & -0.002 & -0.004\\ -0.002 & 0.0008 & -0.001\\ -0.004 & -0.001 & 0.006\end{bmatrix} \qquad (63)$$

$$^{B}J_{outer}=\begin{bmatrix}0.003 & -0.002 & -0.004\\ -0.002 & 0.0004 & -0.001\\ -0.004 & -0.001 & 0.0003\end{bmatrix} \qquad (64)$$

7.1 Test 1 (verification)

The gimbal body is considered as the load of the DC motor. In MATLAB/Simulink, the gimbal body is expressed by its inertia moments. Meanwhile, MATLAB/SimMechanics's tools permit us to represent the gimbal using a different approach. The created gimbal system shown in figure 9 is simulated again using MATLAB/SimMechanics, as shown in figure 10 which clarifies that the base, the outer gimbal and the inner gimbal are represented using the SimMechanics tool. The torques generated in the elevation and azimuth stabilization loops are applied on the inner (elevation) gimbal and the outer (azimuth) gimbal, respectively. Next, the LOS rates are obtained from the gimbals' outputs. The two axes gimbal system responses obtained using both simulations (Simulink and SimMechanics) for the azimuth and elevation channels are displayed in figures 11 and 12, respectively.

It is clear that the responses - obtained using the two simulation approaches - are completely identical in both the elevation and azimuth channels. Therefore, this conformity confirms the model correction and verifies the two axes gimbal system introduced by this research.

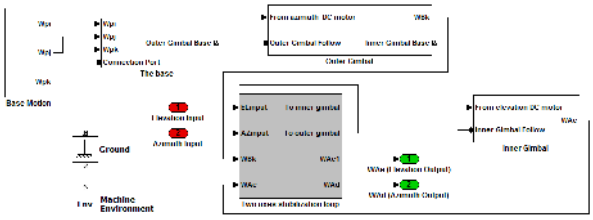

Figure 10. The gimbal modelled by SimMechanics.

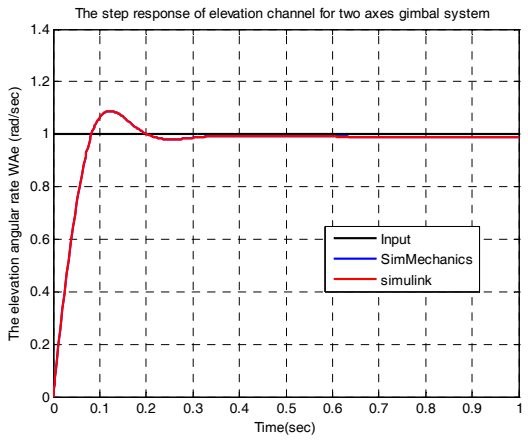

Figure 11. Elevation channel comparison.

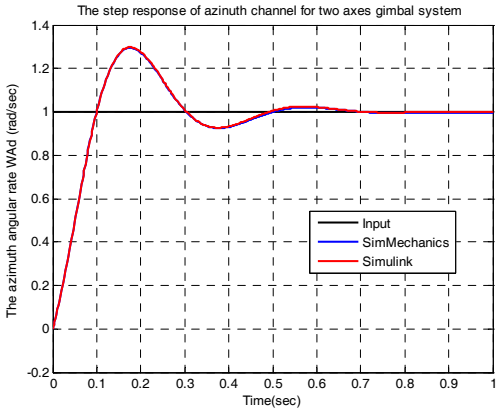

Figure 12. Azimuth channel comparison.

7.2 Test 2 (cross-coupling effect)

It has been explained above that when the base body is non-rotating $\left(\omega_{Pi}=\omega_{Pj}=\omega_{Pk}=0\right)$, the elevation channel (equation 14) is affected by a non-zero disturbance, denoted by:

$$T_{C-EL}=(A_{re}\sin\varepsilon-A_{de}\cos\varepsilon)\dot{\omega}_{Bk} -\frac{1}{2}\left[(A_d-A_r)\sin(2\varepsilon)+2A_{rd}\cos(2\varepsilon)\right]\omega_{Bk}^2 \quad (65)$$

Similarly, the azimuth channel (equation 23) is affected by a non-zero disturbance, denoted by:

$$T_{c-Az}=(A_{re}\sin\varepsilon-A_{de}\cos\varepsilon)\dot{\omega}_{Ae} +(A_{re}\cos\varepsilon+A_{de}\sin\varepsilon)\omega_{Ae}^2 +\left[(A_d-A_r)\sin(2\varepsilon)+2A_{rd}\cos(2\varepsilon)\right]\omega_{Ae}\omega_{Bk} \quad (66)$$

The disturbance terms (65, 66) have been called 'cross-coupling terms'. It is clear that they are independent of the azimuth gimbal's inertia parameters and that they can be eliminated when the next condition is satisfied:

$$\left(A_{re}=A_{de}=A_{rd}=0\,\&\,A_r=A_d\right) \quad (67)$$

On the other hand, when (67) is applied on the elevation motion equation (14), all the disturbance terms caused by the gimbals' inertia parameters and base angular motions are cancelled irrespective of the base motions, such that equation (14) becomes:

$$A_e\dot{\omega}_{Ae}=T_{EL} \quad (68)$$

Equation (68) indicates that only the torque T_{EL} generated by the DC motor will affect the elevation gimbal. Meanwhile, inserting (67) into the azimuth motion equation (23) is not enough to cancel the whole disturbance terms, as is shown in the resulting equation:

$$J_{eq}\dot{\omega}_{Bk}=T_{Az}+T_{d1}+T_{d2} \quad (69)$$

It is realized that the azimuth motion is still affected by the azimuth gimbal's inertia parameters and the base angular motions included in terms T_{d1}, T_{d2}, which were previously indicated in (25) and (26), respectively. Therefore, these remaining disturbances cannot be cancelled unless the base is non-rotating. If it is supposed that $\left(\omega_{Pi}=\omega_{Pj}=\omega_{Pk}=0\right)$, the equation for the azimuth motion (69) becomes:

$$J_{eq}\dot{\omega}_{Bk}=T_{Az} \quad (70)$$

In this case, it can be said that only the torque T_{AZ} generated by the DC motor will affect the azimuth gimbal.

The gimbal system model is tested considering scenarios indicated in table 3 to display the effects of cross-coupling when $\omega_{EL}=\omega_{AZ}=30\,\mathrm{deg/sec}$. The system response for scenario S1 is shown in figures 13 and 14. The other results are included in tables 4 and 5, which show that although illuminating the cross-coupling improves the elevation response from the overshoot viewpoint, the overshoot dramatically increases in the azimuth channel. This phenomenon can be explained as follows. When cross-coupling is ignored utilizing (67), all the disturbances in the elevation channel are cancelled (68); meanwhile, the azimuth gimbal is still affected with torque disturbances due to the gimbals' inertial parameters and base angular motions (69).

Scenario	Base angular velocities (deg/sec)		
	ω_{Pi}	ω_{Pj}	ω_{Pk}
S1	0	0	0
S2	5	5	5
S3	10	15	10
S4	15	30	20
S5	20	40	30
S6	25	50	40
S7	30	60	50
S8	35	70	60
S9	40	80	120

Table 3. Tests scenarios.

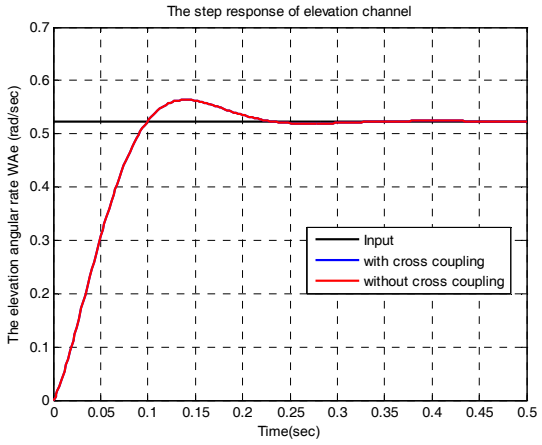

Figure 13. Step response for S1 in the elevation channel.

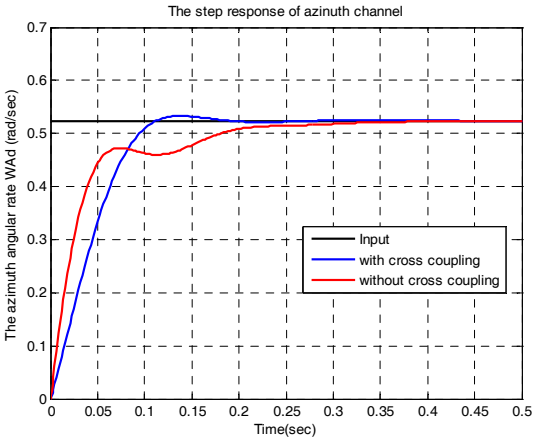

Figure 14. Step response for S1 in the azimuth channel.

Scenario	Response with cross-coupling			
	Elevation		Azimuth	
	t_s (sec)	Overshoot (%)	t_s (sec)	Overshoot (%)
S1	0.225	7.76	0.18	1.89
S2	0.33	8.78	0.25	6.46
S3	0.35	18.76	0.35	11.01
S4	0.3	50.75	0.33	23.63
S5	0.3	77.25	0.3	39.56
S6	0.38	105.74	0.3	56.27
S7	0.45	135.95	0.3	73.15
S8	0.45	167.69	0.45	91.2
S9	0.45	218.74	0.45	203.25

Table 4. Response parameters with cross-coupling.

Scenario	Response without cross-coupling			
	Elevation		Azimuth	
	t_s (sec)	Overshoot (%)	t_s (sec)	Overshoot (%)
S1	0.225	7.76	0.33	0
S2	0.33	8.78	0.3	0
S3	0.35	18.76	0.2	9.25
S4	0.3	49.62	0.25	31.2
S5	0.3	74.88	0.25	54.3
S6	0.38	101.91	0.3	77.74
S7	0.45	129.64	0.3	101.15
S8	0.45	157.93	0.45	124.66
S9	0.45	188.53	0.45	270.36

Table 5. Response parameters without cross-coupling.

7.3 Test 3 (angular base motion effect)

It was proven that the disturbances in both channels are caused by the base rotations and the gimbals' inertial parameters. Thus, it is useful to study how the angular base motion affects the system response considering the gimbals' mass distribution. Therefore, the gimbal system has been tested for two cases under different rates. First, when the gimbals have no dynamic unbalance, and second when the gimbals have dynamic unbalance. The results of this investigation are shown in table 6 when $\omega_{EL} = \omega_{AZ} = 60\text{deg/sec}$. To clarify, figures 15 and 16 show the gimbal system response for S9.

Scenario	Response overshoot (%)			
	Without dynamic unbalance		With dynamic unbalance	
	Elevation	Azimuth	Elevation	Azimuth
S1	7.4	5.25	7.4	0.76
S2	7.64	7.35	7.64	3.05
S3	10.32	9.84	10.22	5.06
S4	19.29	15.28	19.29	9.84
S5	29.9	22.06	29.9	16.14
S6	39.54	29.51	39.54	22.92
S7	51.76	37.63	51.76	30.09
S8	65.62	46.42	65.62	38.11
S9	80.61	101.05	90.44	89.39

Table 6. Effects of the dynamic unbalance and base rates.

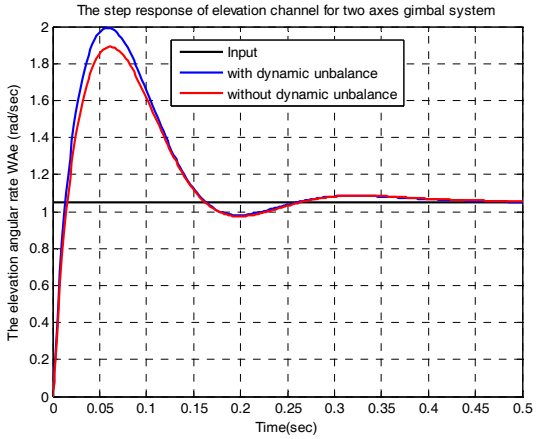

Figure 15. Elevation gimbal response in S9.

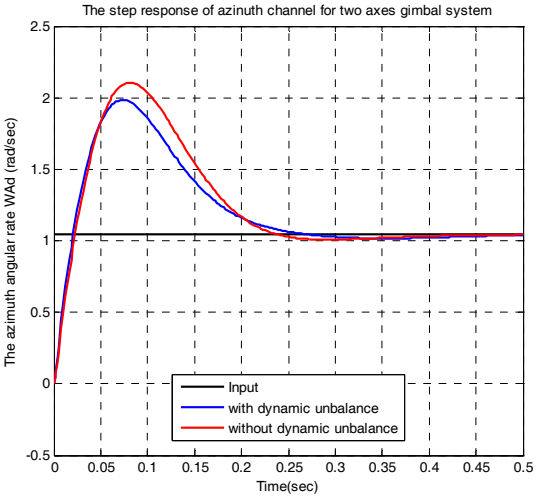

Figure 16. Azimuth gimbal response in S9.

Based on the geometrical properties of the gimbal system shown in figure 1, it can be concluded that the base angular velocities ω_{Pj}, ω_{Pk} are the most dominant rates that basically affect the gimbal system performance. The gimbal system was tested for a wide range of rates and the results indicated in table 6 show that whenever these rates increase the response overshoot dramatically increases. Therefore, it is perhaps necessary to develop the PI controller in such a way as to give better performance with acceptable overshoot under the high values of the base angular velocities. Naturally, the permissible overshoot is defined according to the application for which the gimbal system is used.

8. Conclusion

In this paper, a two axes gimbal system was proposed and formulated utilizing Newton's second law. The construction of the stabilization loop was introduced and the concepts of cross-coupling and dynamic unbalance were accomplished. The equations for the gimbals' motion were derived and introduced in two formulations according to the dynamic mass unbalance. Afterwards, three tests were carried out. At first, the gimbal system was simulated using MATLAB/Simulink and MATLAB/SimMechanics. A comparison between the system responses in the two simulations was made and the comparison results verified the proposed model. Second, the cross-coupling terms in the elevation and azimuth channels were obtained. An investigation was made to show how the cross-coupling affects the system response according to different base rates. The third test was carried out to study the effects of the base rotations on the system response by taking into account the properties of the gimbals' mass distribution. Based on the parametric study made in tests 2 and 3, the following conclusions can be drawn:

1. The overshoot of the gimbal system response with cross-coupling increases in both the elevation and azimuth channels whenever the base rates increase (table 4).
2. When condition (63) is satisfied, the response overshoot in the elevation channel decreased, while the overshoot in the azimuth channel dramatically increased (table 5).
3. The cross-coupling between the elevation and azimuth gimbals is the result of the gimbal geometry, the gimbal assembly parameters and the base motions. Therefore, the cross-coupling relationships are crucial to consider when a two axes gimbal system is designed.
4. The system overshoot largely increases against the high base rates (table 6).

For further future research works, there are two directions. The first direction is to expand the mathematical model of the gimbal system assuming that the gimbals have static mass unbalance, which results from the offset between the origin of the gimbal coordinate system (the gimbal pivot or gimbal rotation axis) and the gimbal mass centre. In addition, the mathematical model can be expanded by taking into account the gimbals' friction. Another interesting future direction is to utilize modern control approaches such as fuzzy logic and neural networks, or a combination of them, to design the control system of a two axes gimbal mechanism. Furthermore, it would be useful and important to develop the controller into an adaptive form so as to overcome the changing of the rates and achieve high performance with acceptable overshoot, making the gimbal system susceptible to be utilized in a dynamic environment which usually imposes variable rates on the base to which the gimbal system is fixed.

9. References

[1] Masten M.K. (2008) Inertially stabilized platform for optical imaging systems. IEEE Control Systems Magazine, Vol. 28, pp. 47-64.

[2] Final report (1976) Analytic study of inside-out / coincident gimbal dynamics. The Bendix Corporation, Guidance System Division.

[3] Stokum L.A. and Carroll G.R. (1984) Precision stabilized platform for ship-borne electro-optical systems. SPIE, Vol. 493, pp. 414-425.

[4] Rue A.K. (1974) Precision stabilization systems. IEEE Trans. Aerospace and Electronic Systems, Vol. AES-10, No. 1, pp. 34-42.

[5] Ekstrand B. (2001) Equation of motion for a two axes gimbal system. IEEE Trans. On Aerospace and Electronic Systems, Vol. 37, No. 3, pp. 1083-1091.

[6] Daniel R. (2008) Mass properties factors in achieving stable imagery from a gimbal mounted camera. Published in SPIE Airborne Intelligence, Surveillance, Reconnaissance (ISR) Systems and Applications V, Vol. 6946, doi:10.1117/12.778245.

[7] Yu S. and Zhao Y. (2010) A New measurement method for unbalanced moments in a two axes gimbaled seeker. Chinese Journal of Aeronautics, Vol. 23, No. 1, pp. 117-122.

[8] Özgür H., Aydan E. and İsmet E. (2011) Proxy-based sliding mode stabilization of a two axes gimbaled platform. Proceedings of the World Congress on Engineering and Computer Science, San Francisco, (WCECS), 19-21 October. Vol. I.

[9] Ravindra S. (2008) Modeling and simulation of the dynamics of a large size stabilized gimbal platform assembly. Asian International Journal of Science and Technology in Production and Manufacturing, Vol. 1, No. 2, pp. 111-119.

[10] Khodadadi H. (2011) Robust control and modeling a 2-DOF Inertial Stabilized Platform. International Conference on Electrical, Control and Computer Engineering, Pahang, Malaysia, June 21-22, pp. 223-228.

[11] Hilkert J.M. (2008) Inertially stabilized platform technology. IEEE Control Systems Magazine, Vol. 28, pp. 26-46.
[12] Tang K.Z., Huang S.N., Tan K.K. and Lee T.H. (2004) Combined PID and adaptive nonlinear control for servo mechanical systems. Mechatronics, Vol. 14, pp. 701-714.
[13] Malhorta R., Singh N. and Singh Y. (2010) Design of embedded hybrid fuzzy-GA control strategy for speed control of DC motor: a servo control case study. International Journal of Computer Applications, Vol. 6, No. 5, pp. 37-46.